

“Thiol-ene” grafting of silica particles with three-dimensional branched copolymer for HILIC/cation-exchange chromatographic separation and N-glycopeptide enrichment

Wenya Shao^{1,2} · Jianxi Liu^{1,2} · Yu Liang¹ · Kaiguang Yang¹ · Yi Min¹ · Xiaodan Zhang¹ · Zhen Liang¹ · Lihua Zhang¹ · Yukui Zhang¹

Received: 30 June 2017 / Revised: 24 August 2017 / Accepted: 6 September 2017 / Published online: 25 September 2017
© Springer-Verlag GmbH Germany 2017

Abstract Three-dimensional branched copolymer, with *N,N'*-methylene bisacrylamide as the crosslinker and 3-allyloxy-2-hydroxy-1-propane sulfonic acid sodium salt as the monomer, was grafted from silica particles by thiol-ene click reaction. The obtained hydrophilic material with sulfonic acid groups was successfully applied for chromatography separation and glycopeptide enrichment. The separation mechanism was proven as the mixed mode of hydrophilic interaction and cation-exchange by investigating the effect of various chromatographic factors on the retention of polar analytes. By such mixed-mode chromatography, nucleosides, nucleobases, and acidic compounds were successfully separated. The column efficiency was up to 136,000 theoretical plates m^{-1} for cytidine, which was much higher than those of previous reports. Furthermore, benefitting from the large amount of hydrophilic groups provided by the branched copolymer, the material was used for the selective enrichment of glycopeptides. Results demonstrated the great potential of such material for chromatography separation and glycoproteome analysis.

Keywords Hydrophilic interaction chromatography · Mixed-mode retention mechanism · Separation · Glycopeptide enrichment · Branched copolymer

Introduction

Hydrophilic interaction liquid chromatography (HILIC) was first named in 1990 [1] and gained increasing interest due to the growing demand for the analysis of polar compounds [2]. The mobile phase of HILIC contains high organic content and relatively modest concentration of volatile salts, highly compatible with electrospray ionization mass spectrometry (ESI-MS) [3]. Furthermore, HILIC is orthogonal to reversed-phase HPLC, enabling the establishment of multidimensional separation for complex sample analysis [4]. Therefore, HILIC has been widely applied in the analysis of pharmaceuticals, metabolomics, and proteomics, for both separation and the selective enrichment of polar components, e.g., glycopeptides [5–10]. To obtain a wide range of selectivity for various compounds and high separation efficiency, the development of HILIC stationary phases has always been a research focus.

However, with bare silica or silica modified with polar entities (such as amino, amide, cyano, and diol groups [11]) as the stationary phase, the column efficiency and the separation resolution of structurally similar analytes still need to be improved [12]. To solve this problem, the introduction of multiple interactions on the separation media is a good strategy [13–16]. Alpert [17] proved that the combination of electrostatic repulsion and hydrophilic interaction (ERLIC) enabled the isocratic resolution of peptides, amino acids, and nucleotides. Qiao et al. developed glucaminium-based ionic liquid stationary phases, which exhibited HILIC/anion-exchange mixed-mode retention mechanism and was

Published in the topical collection celebrating *ABCs 16th Anniversary*.

Electronic supplementary material The online version of this article (<https://doi.org/10.1007/s00216-017-0626-x>) contains supplementary material, which is available to authorized users.

✉ Lihua Zhang
lihuazhang@dicp.ac.cn

¹ Key Laboratory of Separation Science for Analytical Chemistry, National Chromatographic R. & A. Center, Dalian Institute of Chemical Physics, Chinese Academy of Sciences, 457 Zhongshan Road, Dalian, Liaoning 116023, China

² University of Chinese Academy of Sciences, Beijing 100049, China

successfully applied to nucleotides and flavonoid separation [18, 19]. However, the column efficiency was limited since the particles were grafted with monolayer functionalized groups.

Polymer brushes are an advanced structure applied in many fields such as chemical synthesis, material modification, and fabrication of polymer materials, since the flexible polymer chains with three-dimensional (3D) nanostructure can increase the interaction between materials and targets. Various approaches can be employed for polymer materials, e.g., surface-initiated ionic polymerization, living/controlled free polymerizations such as nitroxyl-mediated polymerization (NMP), atom transfer radical polymerization (ATRP), reversible-addition fragmentation chain transfer (RAFT) polymerization [20], and click chemistry. Among various surface-polymerization strategies, thiol-ene surface-initiated click reaction copolymerization [21] is a powerful tool for the synthesis of polymer brushes, due to its excellent specificity, simplicity, high efficiency, and great robustness to oxygen or water [22].

Herein, we developed a HILIC/cation-exchange stationary phase by grafting 3D branched copolymer onto silica particles via thiol-ene click copolymerization, with *N,N'*-methylenebisacrylamide (MBAAm) as the crosslinker, 3-allyloxy-2-hydroxy-1-propanesulfonic acid sodium salt (AHPS) as the monomer, and 2,2'-azobis(2-methylpropionitrile) (AIBN) as the initiator. The 3D ligand provided abundant functional binding sites, which endowed the silica particles with high hydrophilicity and synergetic electrostatically induced hydration. By using Sil@Poly(AHPS-co-MBAAm) particles, nucleosides, nucleobases, and acidic compounds were successfully separated with high efficiency based on the mixed-mode retention mechanism of HILIC and cation-exchange. Furthermore, such materials were also applied to glycopeptide enrichment with high selectivity.

Experimental

Reagent and materials

Porous silica particles (diameter 5 μm , pore size 70 \AA) were purchased from Fuji Silysia Chemical (Aichi, Japan). Bovine serum albumin (BSA, bovine serum) was obtained from Sino-American Biotec (Luoyang, China). PNGase F was bought from New England Biolabs (Ipswich, MA, USA). Dithiothreitol (DTT) and iodoacetamide (IAA) were from Acros (Morris Plains, NJ, USA). Acetonitrile (ACN, HPLC grade) was ordered from Merck (Darmstadt, Germany). Water was purified by a Milli-Q system (Millipore, Milford, MA, USA). (3-Mercaptopropyl)trimethoxysilane (95%), *N,N'*-methylenebisacrylamide (MBAAm, 98%), 3-allyloxy-2-

hydroxy-1-propanesulfonic acid sodium salt solution 40 wt% in H_2O (AHPS), thymidine, uridine, adenosine, cytidine, guanosine, cytosine, thymine, uracil, adenine, phenol, benzoic acid, 4-hydroxybenzoic acid, 3-chlorobenzoic acid, 3,5-dinitrobenzoic acid, 3-nitrobenzoic acid, nicotinamide, pyridoxine, nicotinic acid, ammonium acetate, acetic acid, trypsin (bovine pancreas), IgG (human serum), and trifluoroacetic acid (TFA) were purchased from Sigma-Aldrich (St. Louis, MO, USA).

Synthesis of Sil@Poly(AHPS-co-MBAAm) particles

To introduce the “clickable” groups on the surface of silica particles, 6 g of silica particles was suspended in 50 mL of anhydrous toluene solution, and then 4.3 mL of (3-mercaptopropyl)trimethoxysilane was added into the mixture stirring in a nitrogen atmosphere at room temperature. After refluxed at 110 $^{\circ}\text{C}$ for 24 h, the particles were rinsed successively with dry toluene, methanol, and acetone before dried under vacuum overnight to obtain the SH-modified silica (Sil@SH).

Then, 690.6 mg MBAAm, 2 mL AHPS monomer, and the obtained SH-modified silica beads (2.5 g) were reacted in 100 mL water-methanol (2:3, *v/v*) with 72 mg AIBN as the initiator at 70 $^{\circ}\text{C}$ for 24 h. Finally, the resulting particles were washed with methanol and water to remove the residual monomer and oligomer for three times. After dried under vacuum at 40 $^{\circ}\text{C}$ for 12 h, the prepared Sil@Poly(AHPS-co-MBAAm) particles were collected.

Characterization

Thermogravimetric analysis (TGA) was carried out on a Cahn Thermax 500 instrument (NETZSCH, Selb, Germany) from 35 to 800 $^{\circ}\text{C}$ with a heating rate of 10 $^{\circ}\text{C min}^{-1}$ under flow argon. The zeta potential of particles suspended in 50 mM ammonium formate and formic acid buffer (pH 4) was measured with Malvern Nano Z Zetasizer (Malvern, Worcs, UK). Stock sample solutions were prepared by suspending 1 mg material in 10 mL of buffer. Fourier transform-infrared spectra were collected on a PerkinElmer Spectrum GX spectrometer (San Jose, CA, USA) by mixing polymer particles with KBr and scanning at the range of 400–4000 cm^{-1} . The specific surface area and mesopore size were determined by nitrogen adsorption-desorption measurements (QuadraSorb SI4, FL, USA), and obtained from the isotherms by the BET and DFT methods, respectively. The morphology of the particles was observed by scanning electron microscopy (SEM) after sputtering gold layers for 120 s (20 kV SEM, FEI, EIN, Holland).

Sample preparation

All the small molecules used for separation were dissolved in ACN/H₂O (85/15, v/v). The concentration of standard solutions was 50 µg mL⁻¹ for nucleosides, nucleobases, and vitamins and 10–50 µg mL⁻¹ for acidic solutes.

IgG and BSA digests were separately prepared according to a previous protocol [23]. Proteins were dissolved in denaturing buffer (8 M urea), reduced in 100 mM DTT at 56 °C for 1.5 h, and alkylated by 200 mM IAA for 40 min at room temperature in the dark. The solution was diluted tenfold with 50 mM NH₄HCO₃ buffer (pH 8.0) and then digested with trypsin (enzyme/protein ratio of 1:50, m/m) at 37 °C for 12 h. The tryptic digested peptides were desalted by home-made C18 precolumn, lyophilized, and stored at -20 °C for usage.

Column packing and chromatography conditions

The Sil@Poly(AHPS-co-MBAAm) particles were packed into either a stainless steel tube (150 mm × 4.6 mm i.d.) or a PEEK tube (50 mm × 0.3 mm i.d.), using methanol as the propulsive solvent at a constant pressure of 60 MPa. Separation was performed on an HPLC instrument with a diode array detector (Chromaster HPLC, Hitachi High-Tech, Tokyo, Japan) with a stainless steel column. The flow rate was 1.00 mL min⁻¹. The detection wavelength was set at 254 nm, the injection volume was 5 µL, and the column temperature was controlled at 25 °C. The mobile phase consisted of ammonium acetate (NH₄Ac) buffer and ACN. The retention time of methanol was used as the dead time (t_0). The retention factor (k) was calculated by the equation: $k = (t_R - t_0)/t_0$, where t_R is the retention time of the analyte. The column was equilibrated by initial mobile phase for 40 min until a stable baseline is achieved.

Glycopeptide enrichment

Glycopeptide enrichment was performed by an UltiMate 3000 pump (Dionex, Sunnyvale, CA, USA) using a PEEK column, following the previous protocol [24] but with minor modification. The mixture of 1 µg IgG digests and BSA digests (1:10, 1:100, m/m) was redissolved in ACN/H₂O/FA (75/25/0.1) and then loaded onto the column at the flow rate of 15 µL/min. Nonglycopeptides were removed by rinsing with ACN/H₂O/FA (75/25/0.1, v/v/v), while the glycopeptides were eluted with ACN/H₂O/FA (0/100/0.1, v/v/v). Then, 2 µL of enriched glycopeptides solution and the same volume of 2,5-dihydroxybenzoic acid (DHB) solution (20 mg mL⁻¹, 0.1% TFA in 60% ACN aqueous solution) were sequentially dropped onto a MALDI plate and analyzed by matrix-assisted laser desorption ionization-time-of-flight mass spectrometry (MALDI-TOF MS, Bruker, Daltonios, Germany).

Others were dried and redissolved in 20 µL NH₄HCO₃ solutions (50 mM), further deglycosylated by PNGase F (50,000 U mol⁻¹), and subjected to MALDI-TOF MS. Experiments were performed on Bruker Ultraflex III MALDI-TOF/TOF MS instrument (Bruker, Daltonios, Germany). The primary samples without enrichment were also analyzed by MALDI-TOF MS.

Results and discussion

Synthesis and characterization of Sil@Poly(AHPS-co-MBAAm) particles

The preparation of branched copolymer-modified silica particles is shown in Scheme S1 in the Electronic Supplementary Material (ESM). Beneficial from the facile and efficient thiol-ene click copolymerization reaction [25], high active ends of the monomers, and the use of MBAAm as the crosslinker, the branched copolymer structure was formed by a one-step reaction, in which the large amount of amide groups and hydroxyl groups could enhance hydrophilicity and the sulfonate groups could provide cation-exchange interaction.

The morphology and the components of the prepared Sil@Poly(AHPS-co-MBAAm) materials were characterized. As shown in the SEM image (Fig. 1a), a layer of floccule on the surface of Sil@Poly(AHPS-co-MBAAm) particles could be observed, indicating that the branched copolymers were grafted on the silica particle surface. Besides, the particle was still monodispersed, uniform, and highly spherical, playing an important role to ensure high separation efficiency. The nitrogen adsorption-desorption analysis (shown in Fig. 1b) revealed that the mesopore size of silica particles decreased from 6.8 to 5.9 nm after clicking branched copolymer, demonstrating the successful modification of a dense layer of branched copolymer on the mesopore wall without blocking the mesopores. Compared with unmodified Sil@SH particles, the pore size distribution was narrower, indicating that the surface modification improved the homogeneity of porous structure, beneficial to improve the separation performance. Thermogravimetric analysis was further performed. As shown in Fig. 1c, regarding the mass loss of Sil@SH and Sil@Poly(AHPS-co-MBAAm) between 200 and 600 °C, the loss of the molecules from silica substrates [26], was 8 and 21%, respectively, which further confirmed the modification of the copolymer. The Fourier transform-infrared (FT-IR) spectroscopy analysis also demonstrated the successful synthesis of Sil@Poly(AHPS-co-MBAAm) particles, in Fig. 1d, since the peak at 1673 cm⁻¹ was attributed to C=O stretching vibration, the characteristic bands at 1542 cm⁻¹ was assigned to N-H bending vibration and C-N stretching vibration of amide group in MBAAm, and the peak emerged at 694 cm⁻¹ was the characteristic vibration of C-S in APHS.

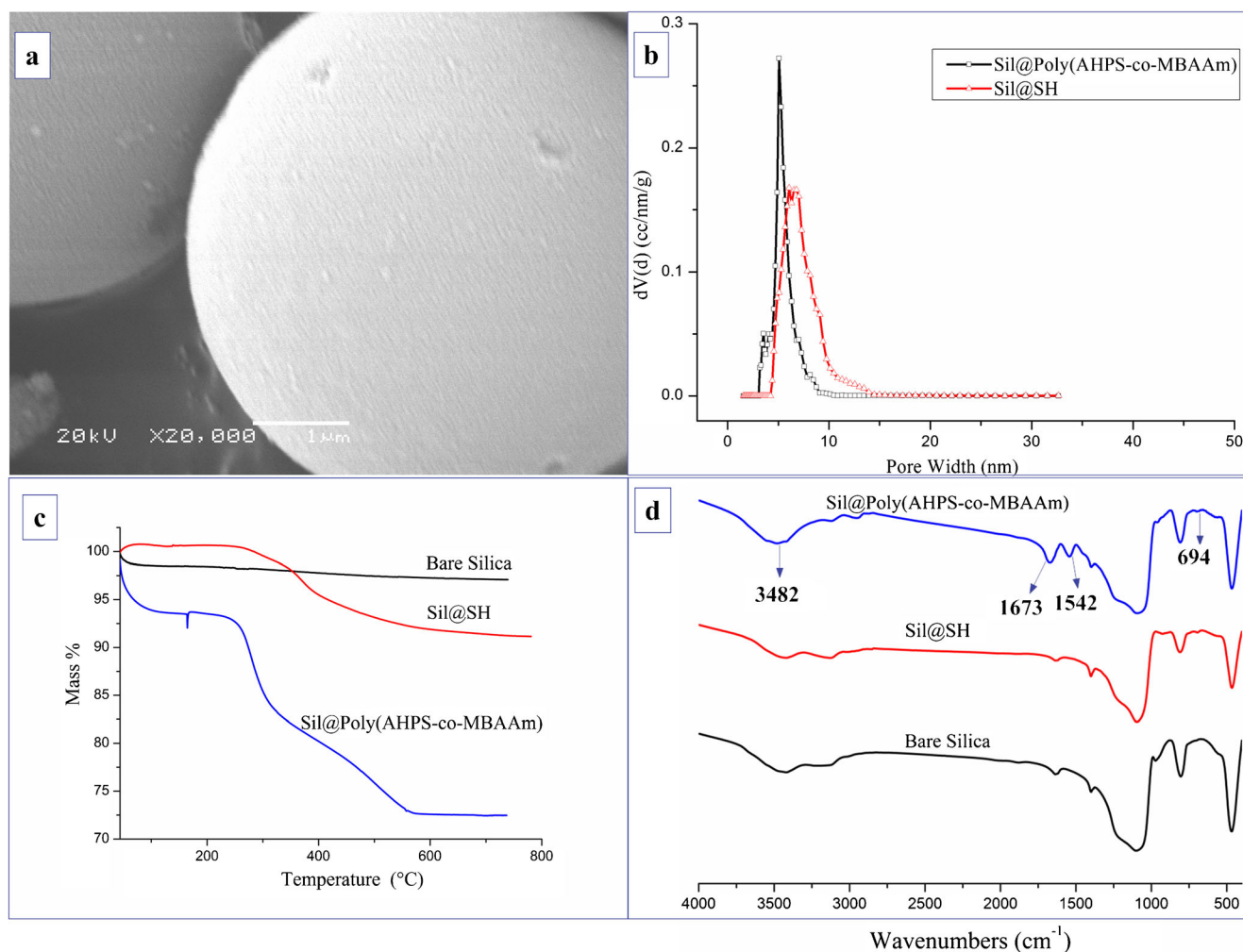


Fig. 1 **a** SEM images of Sil@Poly(AHPS-co-MBAAm). **b** DFT adsorption pore size distribution. **c** TG analysis. **d** FT-IR spectra

The Zetasizer photon spectrometer was employed to evaluate the surface charge properties of Sil@Poly(AHPS-co-MBAAm) particles dispersed in 50 mM ammonium formate and formic acid buffer (pH 4). For bare silica, the ζ potential was -5.98 mV, because of silanol groups on the surface. After modification by mercaptopropyl, the ζ potential became -8.6 mV, contributed by the attached thiol group. For Sil@Poly(AHPS-co-MBAAm) particles, the ζ potential was decreased to -31.2 mV, mainly contributed by the large amount of sulfonate groups. The carbon load and the sulfur load were estimated further by elemental analyses (see ESM Table S1).

All the abovementioned characterization confirmed the synthesis of branched copolymer Sil@Poly(AHPS-co-MBAAm) particles by thiol-ene click copolymerization.

Effect of mobile phase on retention behavior

The effects of ACN content, salt concentration, and pH of mobile phase on the retention behavior of nucleotides and

acidic compounds (the pK_a values listed in Fig. S1 in the ESM) on the Sil@Poly(AHPS-co-MBAAm) packed column were investigated to reveal the separation mechanism.

In this study, the effect of ACN content on the retention of analytes was investigated with the volume fraction ranging from 65 to 90%. As shown in Fig. 2a, b, the retention of all analytes was increased with the ACN content, which demonstrates the typical HILIC retention mechanism, contributed by the partitioning between the semi-immobilized aqueous layer on the surface of stationary phase and the mobile phase [27].

Ammonium acetate was added in the buffer due to its good solubility in mobile phase containing high organic solvent content, and the effect of salt concentration was investigated by varying the salt concentration from 5 to 30 mM dissolved in 85% ACN (pH 4.37). For charged HILIC stationary phases, salt concentration affects the hydrophilic partition and ion-exchange process. On the one hand, higher salt concentration may generate more ions into the semi-immobilized aqueous layer formed on the stationary phase, leading to the larger volume of the water layer and the improvement on retention.

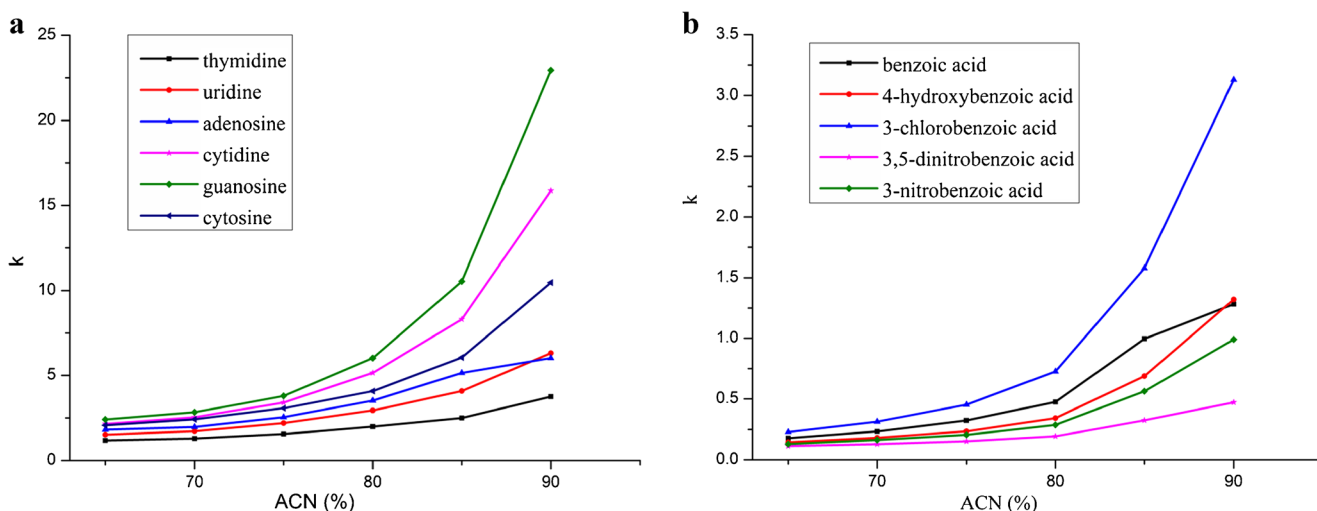


Fig. 2 The effect of water content on the retention factors (a) nucleosides and nucleobases and (b) acidic compounds. Mobile phases with different volume ratios of ACN and H₂O contained 15 mM ammonium acetate. *T* = 25 °C; flow rate = 1 mL min⁻¹; UV detection, λ = 254 nm

On the other hand, with the increase of salt concentration, the electrostatic interaction between the stationary phase and the analytes is weakened. For most of nucleotides and nucleobases, which are electrically neutral, the retention factors change slightly with the increased salt concentration (Fig. 3a), but the retention of cytidine, guanosine, and adenine, with strong basicity, becomes weak with the increase of salt concentration, because the electrostatic attraction between such analytes and sulfonate ions plays a control role in separation in low salt concentration. In Fig. 3b, the retention of phenol (*pK_a* 9.95) is almost invariable because the phenol keeps in molecular form at pH 4.37 and the retention is not affected by ion-exchange interaction. Moreover, the retention of other hydrolyzed substituted benzoic acids and substituted

benzoic acids substantially increases with the rising of salt concentration because of the decrease of electrostatic repulsion.

The pH values of the mobile phase could also affect the retention behavior of analytes, mainly through altering the ionization of the analytes and/or the polar groups of the stationary phase. Ammonium acetate was added in the buffer to adjust the pH values. As shown in Fig. 4a, with pH ranging from 3.7 to 7.0, the retention factors of nonionic solutes including nucleosides remain unchanged, consistent with the previous report about HILIC-type columns [28]. Water-soluble vitamins and acidic compounds display different retention trends based on the *pK_a* values (Fig. 4b). For nicotinic acid (*pK_a* 4.75) and pyridoxine (*pK_{a1}* 5.0), the main existing

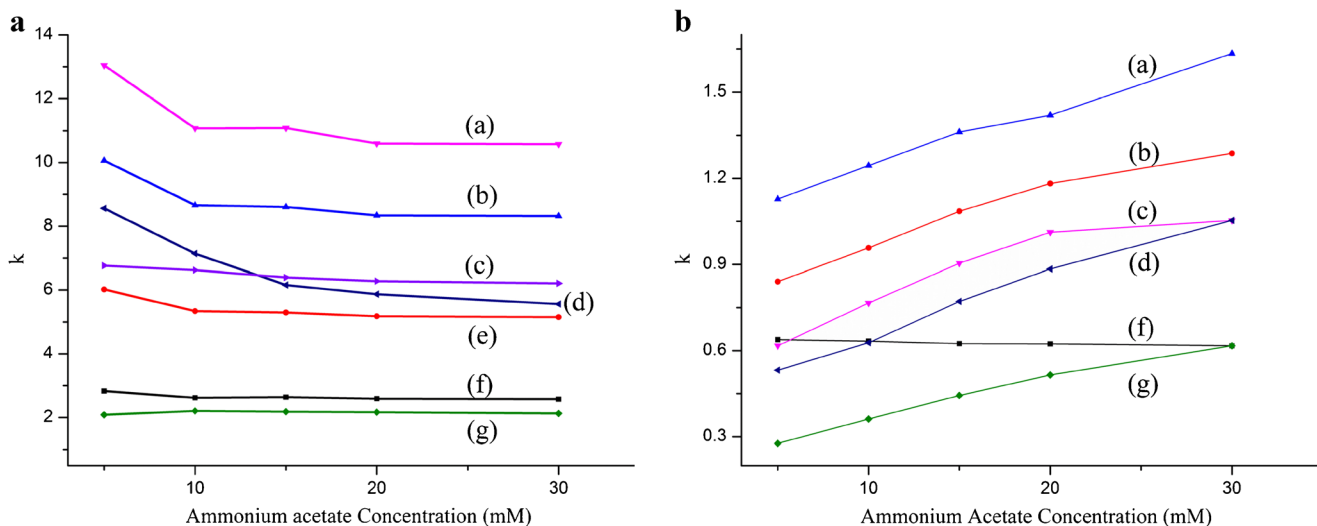


Fig. 3 The effect of ammonium acetate concentration on the retention factors. **a** Nucleosides and nucleobases: (a) guanosine, (b) cytidine, (c) cytosine, (d) adenine, (e) adenosine, (f) thymidine, and (g) thymine. **b** Acids: (a) 4-hydroxybenzoic acid, (b) benzoic acid, (c) 3-chlorobenzoic

acid, (d) 3-nitrobenzoic acid, (f) phenol, and (g) 3,5-dinitrobenzoic acid. Mobile phases of ACN/H₂O (85/15, *v/v*) contained different concentrations of salt. Other chromatographic conditions were the same as Fig. 2

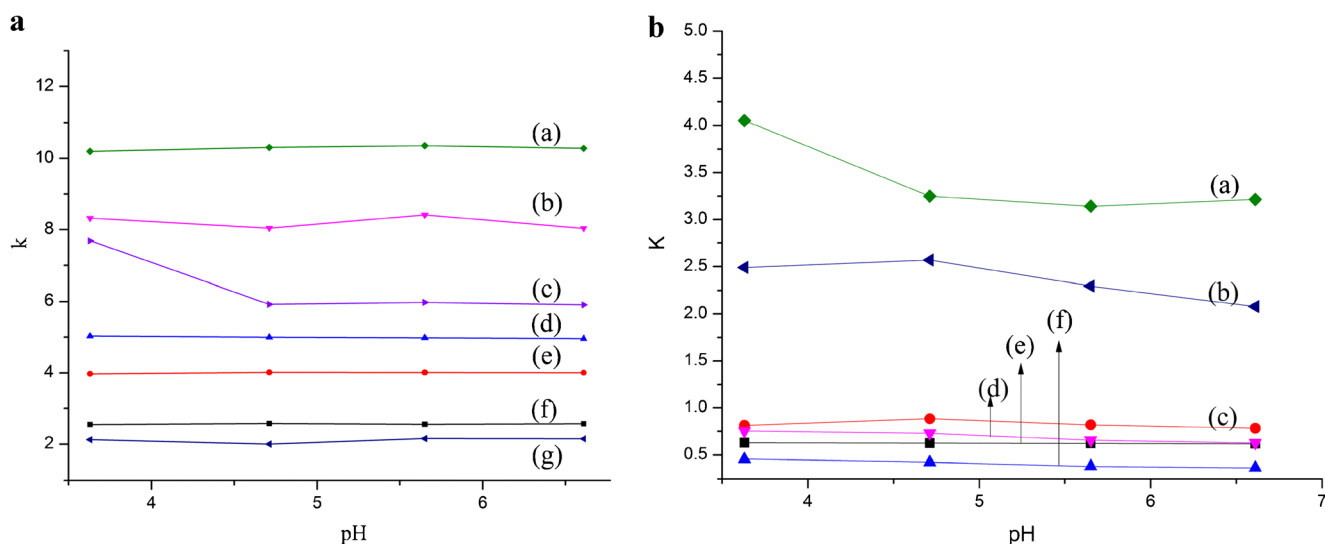


Fig. 4 The effect of pH on the retention factors. **a** Nucleosides and nucleobases: (a) guanosine, (b) cytidine, (c) cytosine, (d) adenosine, (e) uridine, (f) thymidine, and (g) thymine. **b** Acids: (a) pyridoxine, (b) nicotinic acid, (c) 3-chlorobenzoic acid, (d) 3-nitrobenzoic acid, (e)

phenol, and (f) 3,5-dinitrobenzoic acid. Mobile phases with different pH values of ACN/H₂O (85/15, v/v) contained 15 mM ammonium acetate. Other chromatographic conditions were the same as Fig. 2

forms change from molecules to anion within the studied pH range, so the retentions decrease due to the stronger electrostatic repulsion interactions with pH increased. For 3,5-dinitrobenzoic acid (pK_a 2.77), 3-nitrobenzoic (pK_a 3.44), and 3-chlorobenzoic acid (pK_a 3.97), the retention factors change little because they keep in anion forms at pH 3.7–7.0.

The abovementioned results demonstrated that Sil@Poly(MBAAm-co-AHPS) had the mixed-mode mechanism of HILIC and cation-exchange for chromatography separation.

Separation performance

Since the 3D branched copolymer structure of Sil@Poly(MBAAm-co-AHPS) particles can provide abundant water-enriched layer and multiple synergistic effect, the

column efficiency tested by cytidine could reach 136,000 theoretical plates m^{-1} with the mobile phase composed of 20 mM NH₄Ac/ACN (15/85, v/v), higher than previously reported results (75,000 [29] and 80,000 plates m^{-1} [30]).

To demonstrate the separation capacity of our developed Sil@Poly(AHPS-co-MBAAm) stationary phase, the separation of weak basic, basic, and acidic compounds was performed under the optimized conditions. Meanwhile, the separation and retention behaviors were compared under the same condition. As shown in Fig. 5a, the baseline separation of six nucleosides and nucleobases was achieved with symmetrical peak shape in Sil@Poly(AHPS-co-MBAAm) column, which showed better peak shape than the commercial HILIC columns and those previously reported [31]. The retention factors were 4.4, 5.7 and 3.5, 4.4, respectively, for cytosine and cytidine of the two commercial columns

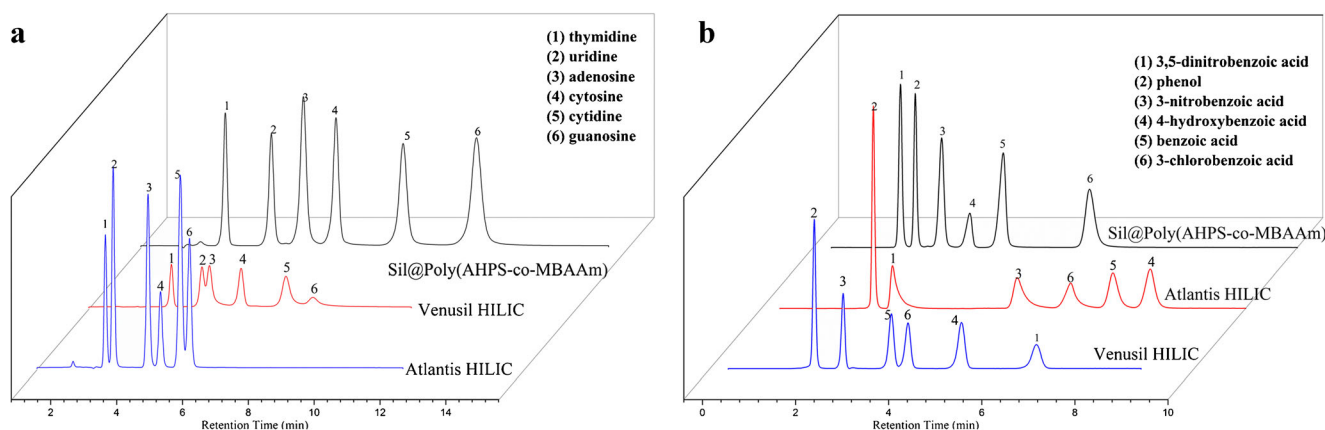


Fig. 5 Separation of **a** nucleosides and nucleobases and **b** acidic compounds on different HILIC columns (150 mm × 4.6 mm i.d.). Separation conditions: $T = 25$ °C; flow rate = 1 mL min^{-1} ; UV

detection, $\lambda = 254$ nm; mobile phase containing 15 mM ammonium acetate, pH 7.38, for **a** ACN/H₂O (85/15, v/v) and for **b** ACN/H₂O (94/6, v/v)

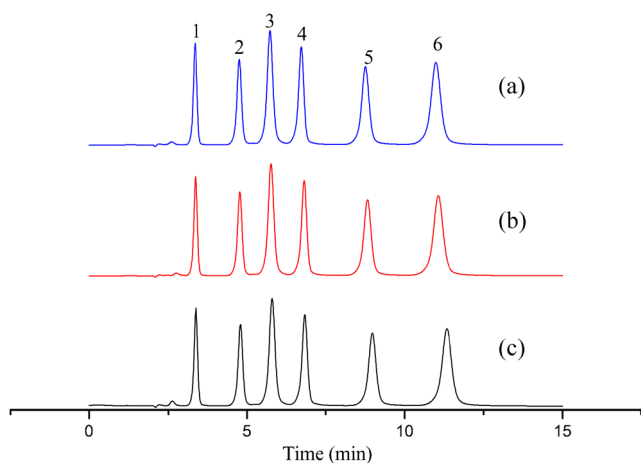


Fig. 6 Mobile phase: ACN/H₂O (85/15, v/v) containing 15 mM ammonium acetate. Peaks: (1) thymidine, (2) uridine, (3) adenosine, (4) cytosine, (5) cytidine, and (6) guanosine. Other chromatographic conditions were the same as Fig. 5

(Venusil HILIC and Atlantis HILIC), while the Sil@Poly(THMA-co-MBAAm) column exhibited much larger retention factors (6.1 and 8.3, respectively) for cytosine and cytidine. It indicated that superior hydrophilicity was achieved by the branched polymer stationary phase. For phenol and other five substituted benzoic acids which were hardly separated in good peak shape due to the complicated forces, they also could be separated quite well in 6 min (Fig. 5b). Compared with the commercial HILIC columns, the Sil@Poly(AHPS-co-MBAAm) column presented different retentions for acidic compound due to the electrostatic repulsion interactions between acidic compounds and sulfonate groups.

The reproducibility was examined using the model compounds thymidine, uridine, adenosine, cytosine, cytidine, and guanosine by injecting three times. Figure 6 shows separation behavior, among which (a) and (b) were two continuous injections. After working for 500 h in 12 months, the column

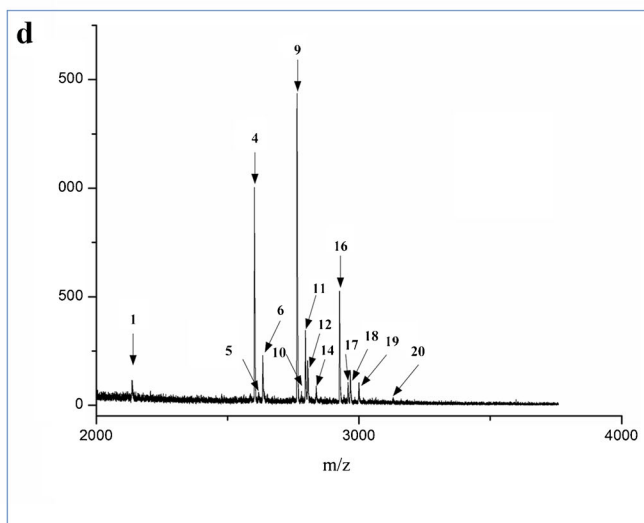
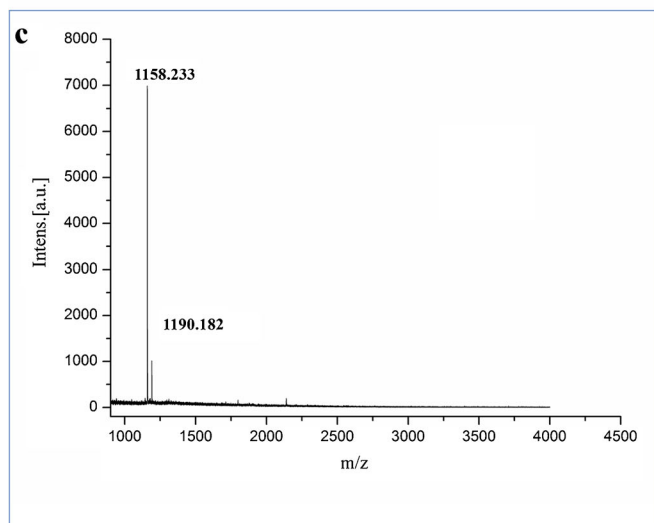
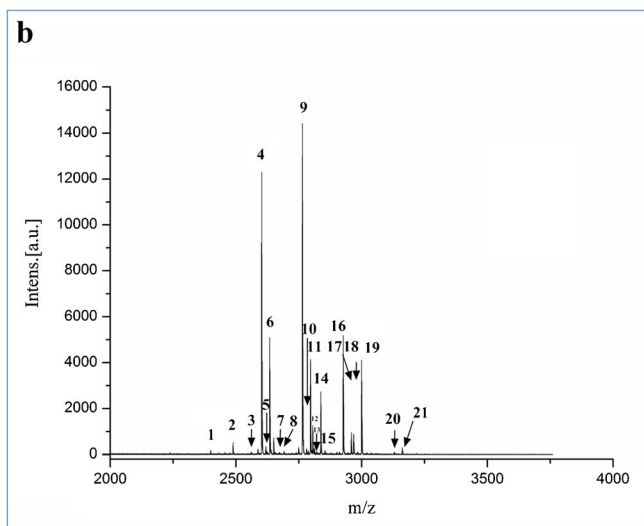
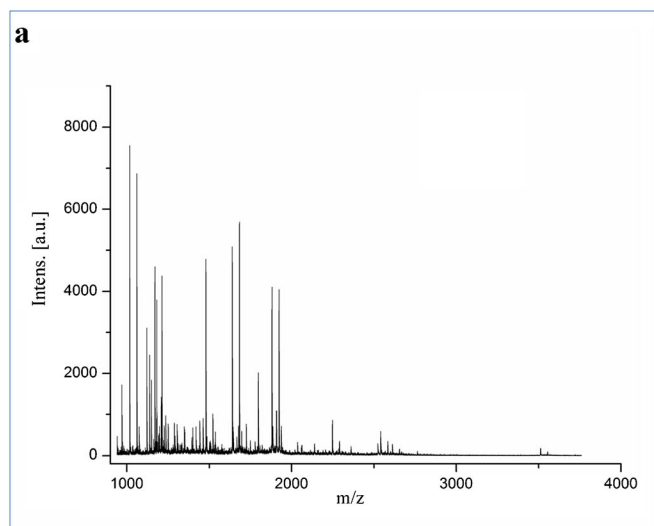


Fig. 7 MALDI-TOF-MS spectra of the mixture of human IgG and BSA digests **a** without enrichment; **b** after enrichment with the Sil@Poly(AHPS-co-MBAAm) packed HILIC column, with a mass

ratio of 1:10 (BSA mass was 1 μg); **c** after treatment with PNGase F (for 24 h at 37 °C); and **d** after enrichment with a mass ratio of 1:100

was repeatedly applied for separation (c). There was no obvious changes of retention time and peak symmetry, indicating that this Sil@Poly(AHPS-co-MBAAm) column exhibited good reproducibility during the HPLC application.

Glycopeptide enrichment

In view of the abundant hydrophilic groups on the branched copolymer of Sil@Poly(AHPS-co-MBAAm) particles, the enrichment of glycopeptides was carried out by HILIC. For the mixture of the tryptic digests of IgG and BSA at a mass ratio of 1:10, as shown in Fig. 7a, without enrichment, the signal of glycopeptides on the MALDI-TOF MS/MS spectra is seriously suppressed by nonglycopeptides. However, after enrichment, 21 glycopeptides (listed on Table S2 in the ESM) of IgG were identified (Fig. 7b), and the detail of each glycopeptide was analyzed by flexAnalysis Version 3.3 and based on a previous work [23]. For the click maltose HILIC column, which was widely used for glycopeptide enrichment, by using the same enrichment strategy, only 11 glycopeptides of IgG were identified [24]. It demonstrated that the Sil@Poly(AHPS-co-MBAAm) packed column exhibits improved glycopeptide capture ability. By further deglycosylation with PNGase F, two deamidated peptides at m/z 1158.2 and 1190.2 with sequences of EEQFN#STFR and EEQYN#STYR were detected without other interference peaks (Fig. 7c), which further confirmed the high enrichment selectivity for the Sil@Poly(AHPS-co-MBAAm) packed column. The unenriched sample was also deglycosylated with PNGase F. The result is shown in Fig. S2 (see ESM). The prepared materials were further evaluated by capturing glycopeptides from the digest mixture of IgG and BSA at a mass ratio of 1:100. As shown in Fig. 7d, 14 glycopeptides were still identified with the same S/N as 10, which demonstrated high selectivity. The unenriched sample was also analyzed by MALDI-TOF MS. The result is shown in Fig. S3 (see ESM).

Conclusions

In summary, we successfully prepared the novel HILIC/cation-exchange particles via thiol-ene click copolymerization reaction. Beneficial from the high hydrophilicity and synergistic multiple effect assisted by the 3D branched copolymer on the surface of silica, the Sil@Poly(AHPS-co-MBAAm) packed column presented good separation performance with column efficiency up to 136,000 theoretic plates m^{-1} , with the mixed-mode retention mechanism of HILIC and cation-exchange. Furthermore, such materials were successfully applied into the selective enrichment of glycopeptides. All these results demonstrate the great potential of the Sil@Poly(AHPS-co-MBAAm) particles in the separation

of polar compounds and the enrichment of glycopeptides. Moreover, this strategy to modify materials with branched copolymer via thiol-ene click copolymerization is promising for designing functionalized materials.

Funding information The authors gratefully acknowledge the financial support from the National Natural Science Foundation of China (21235005, 91543201, 21575139), the National Basic Research Program of China (2012CB910601), and the Creative Research Group Project by NSFC (21321064).

Compliance with ethical standards

Conflict of interest The authors declare that they have no conflicts of interest.

References

- Alpert AJ. Hydrophilic-interaction chromatography for the separation of peptides, nucleic-acids and other polar compounds. *J Chromatogr.* 1990;499:177–96.
- Guo Y. Recent progress in the fundamental understanding of hydrophilic interaction chromatography (HILIC). *Analyst.* 2015;140(19):6452–66.
- Kivilompolo M, Ohrnberg L, Oresic M, Hyotylainen T. Rapid quantitative analysis of carnitine and acylcarnitines by ultra-high performance-hydrophilic interaction liquid chromatography-tandem mass spectrometry. *J Chromatogr A.* 2013;1292:189–94.
- Gama MR, da Costa Silva RG, Collins CH, Bottoli CBG. Hydrophilic interaction chromatography. *TrAC Trends Anal Chem.* 2012;37:48–60.
- Long Z, Guo Z, Liu X, Zhang Q, Liu X, Jin Y, et al. A sensitive non-derivatization method for apramycin and impurities analysis using hydrophilic interaction liquid chromatography and charged aerosol detection. *Talanta.* 2016;146:423–9.
- Creek DJ, Jankevics A, Breitling R, Watson DG, Barrett MP, Burgess KE. Toward global metabolomics analysis with hydrophilic interaction liquid chromatography-mass spectrometry: improved metabolite identification by retention time prediction. *Anal Chem.* 2011;83(22):8703–10.
- Scott NE, Marzook NB, Cain JA, Solis N, Thaysen-Andersen M, Djordjevic SP, et al. Comparative proteomics and glycoproteomics reveal increased N-linked glycosylation and relaxed sequon specificity in *Campylobacter jejuni* NCTC11168 O. *J Proteome Res.* 2014;13(11):5136–50.
- Tetaz T, Detzner S, Friedlein A, Molitor B, Mary JL. Hydrophilic interaction chromatography of intact, soluble proteins. *J Chromatogr A.* 2011;1218(35):5892–6.
- Alagesan K, Khilji SK, Kolarich D. It is all about the solvent: on the importance of the mobile phase for ZIC-HILIC glycopeptide enrichment. *Anal Bioanal Chem.* 2017;409(2):529–38.
- Planinc A, Dejaegher B, Vander Heyden Y, Viaene J, Van Praet S, Rappé F, et al. LC-MS analysis combined with principal component analysis and soft independent modelling by class analogy for a better detection of changes in N-glycosylation profiles of therapeutic glycoproteins. *Anal Bioanal Chem.* 2017;409(2):477–85.
- Buszewski B, Noga S. Hydrophilic interaction liquid chromatography (HILIC)—a powerful separation technique. *Anal Bioanal Chem.* 2012;402(1):231–47.
- Chester TL. Recent developments in high-performance liquid chromatography stationary phases. *Anal Chem.* 2013;85(2):579–89.

13. Qiu H, Takafuji M, Sawada T, Liu X, Jiang S, Ihara H. New strategy for drastic enhancement of selectivity via chemical modification of counter anions in ionic liquid polymer phase. *Chem Commun (Camb)*. 2010;46(46):8740–2.
14. Qiu H, Zhang M, Gu T, Takafuji M, Ihara H. A sulfonic-azobenzene-grafted silica amphiphilic material: a versatile stationary phase for mixed-mode chromatography. *Chem Eur J*. 2013;19(52):18004–10.
15. Shi X, Qiao L, Xu G. Recent development of ionic liquid stationary phases for liquid chromatography. *J Chromatogr A*. 2015;1420:1–15.
16. Jung HR, Sidoli S, Haldbø S, Sprenger RR, Schwammle V, Pasini D, et al. Precision mapping of coexisting modifications in histone H3 tails from embryonic stem cells by ETD-MS/MS. *Anal Chem*. 2013;85(17):8232–9.
17. Alpert AJ. Electrostatic repulsion hydrophilic interaction chromatography for isocratic separation of charged solutes and selective isolation of phosphopeptides. *Anal Chem*. 2008;80(1):62–76.
18. Qiao L, Wang S, Li H, Shan Y, Dou A, Shi X, et al. A novel surface-confined glucaminium-based ionic liquid stationary phase for hydrophilic interaction/anion-exchange mixed-mode chromatography. *J Chromatogr A*. 2014;1360:240–7.
19. Vass A, Robles-Molina J, Perez-Ortega P, Gilbert-Lopez B, Demovics M, Molina-Diaz A, et al. Study of different HILIC, mixed-mode, and other aqueous normal-phase approaches for the liquid chromatography/mass spectrometry-based determination of challenging polar pesticides. *Anal Bioanal Chem*. 2016;408(18):4857–69.
20. Barsbay M, Guven O, Davis TP, Barner-Kowollik C, Barner L. RAFT-mediated polymerization and grafting of sodium 4-styrenesulfonate from cellulose initiated via gamma-radiation. *Polymer*. 2009;50(4):973–82.
21. Liu JX, Yang KG, Shao WY, Qu YY, Li SW, Wu Q, et al. Boronic acid-functionalized particles with flexible three-dimensional polymer branch for highly specific recognition of glycoproteins. *ACS Appl Mater Interfaces*. 2016;8(15):9552–6.
22. Tucker-Schwartz AK, Farrell RA, Garrell RL. Thiol-ene click reaction as a general route to functional trialkoxysilanes for surface coating applications. *J Am Chem Soc*. 2011;133(29):11026–9.
23. Weng Y, Qu Y, Jiang H, Wu Q, Zhang L, Yuan H, et al. An integrated sample pretreatment platform for quantitative N-glycoproteome analysis with combination of on-line glycopeptide enrichment, deglycosylation and dimethyl labeling. *Anal Chim Acta*. 2014;833:1–8.
24. Qu Y, Xia S, Yuan H, Wu Q, Li M, Zou L, et al. Integrated sample pretreatment system for N-linked glycosylation site profiling with combination of hydrophilic interaction chromatography and PNGase F immobilized enzymatic reactor via a strong cation exchange precolumn. *Anal Chem*. 2011;83(19):7457–63.
25. Povie G, Tran AT, Bonnaffe D, Habegger J, Hu Z, Le Narvor C, et al. Repairing the thiol-ene coupling reaction. *Angew Chem*. 2014;53(15):3894–8.
26. Qiu H, Mallik AK, Takafuji M, Liu X, Jiang S, Ihara H. A new imidazolium-embedded C18 stationary phase with enhanced performance in reversed-phase liquid chromatography. *Anal Chim Acta*. 2012;738:95–101.
27. Hemström P, Irgum K. Hydrophilic interaction chromatography. *J Sep Sci*. 2006;29(12):1784–821.
28. Guo Y, Gaiki S. Retention and selectivity of stationary phases for hydrophilic interaction chromatography. *J Chromatogr A*. 2011;1218(35):5920–38.
29. Shen A, Guo Z, Yu L, Cao L, Liang X. A novel zwitterionic HILIC stationary phase based on “thiol-ene” click chemistry between cysteine and vinyl silica. *Chem Commun (Camb)*. 2011;47(15):4550–2.
30. Qiao X, Zhang L, Zhang N, Wang X, Qin X, Yan H, et al. Imidazolium embedded C8 based stationary phase for simultaneous reversed-phase/hydrophilic interaction mixed-mode chromatography. *J Chromatogr A*. 2015;1400:107–16.
31. Padivitage NLT, Armstrong DW. Sulfonated cyclofructan 6 based stationary phase for hydrophilic interaction chromatography. *J Sep Sci*. 2011;34(14):1636–47.